A Low Mach Two-speed Relaxation Scheme for Ideal MHD Equations

Claudius Birke[1] and Christian Klingenberg[1]

Department of Mathematics, University of Würzburg, Germany
claudius.birke@mathematik.uni-wuerzburg.de

Abstract. In this work we apply the two-speed relaxation technique to a relaxation system for the compressible ideal magnethydrodynamic (MHD) equations. We show that the resulting approximate Riemann solver reduces the dissipation in the low Mach regime and can thus generate accurate solutions in this regime even on coarse grids. These findings are supported by numerical results.

Keywords: finite volume methods, relaxation methods, approximate Riemann solver, low Mach regime

1 Introduction

In practical applications such as the simulation of gas flows in the interior of stars, flows with large scale differences can occur. One example is the low sonic Mach number regime, in which the sound speed is much higher than the speed of the fluid flow. Numerically, for finite volume methods two difficulties arise in the low Mach regime: excessive dissipation and a restrictive CFL condition. Basically, there are two strategies in the literature to deal with these challenges:

1. Introduce a low Mach fix in the numerical flux function to reduce the dissipation and use an implicit time integration to overcome the restrictive CFL condition [9, 11].
2. Perform a splitting into convective and acoustic parts and solve the acoustic parts implicitly [8, 7].

In this paper, we focus only on the first strategy and therein only on the design of the numerical flux function. Typically, from implementing a low Mach fix follows that the solver does not satisfy a discrete entropy inequality anymore. This is different for the two-speed relaxation technique. As already shown for isentropic Euler [3], full Euler [4] and full Euler equations with gravity [2], the resulting approximate Riemann solver reduces dissipation in the low Mach regime and still satisfies a discrete entropy inequality. In the spirit of these papers, we apply the two-speed technique to an existing relaxation system for the ideal MHD equations [5, 6]. In a first step we show how the artificial dissipation is reduced in the low Mach regime and substantiate this theoretical result in numerical tests. We assume that the approximate Riemann solver satisfies a discrete entropy inequality as in previous work, but do not show it here. This is left to future work.

2 MHD equations

The compressible ideal MHD equations can be written as

$$\begin{aligned} \frac{\partial \rho}{\partial t} + \nabla \cdot (\rho \boldsymbol{U}) &= 0, \\ \frac{\partial (\rho \boldsymbol{U})}{\partial t} + \nabla \cdot [\rho \boldsymbol{U} \otimes \boldsymbol{U} + (p + \frac{1}{2}|\boldsymbol{B}|^2)\boldsymbol{I} - \boldsymbol{B} \otimes \boldsymbol{B}] &= \boldsymbol{0}, \\ \frac{\partial E}{\partial t} + \nabla \cdot [(E + p + \frac{1}{2}|\boldsymbol{B}|^2)\boldsymbol{U} - \boldsymbol{B}(\boldsymbol{B} \cdot \boldsymbol{U})] &= 0, \\ \frac{\partial \boldsymbol{B}}{\partial t} + \nabla \cdot (\boldsymbol{U} \otimes \boldsymbol{B} - \boldsymbol{B} \otimes \boldsymbol{U}) &= \boldsymbol{0}, \end{aligned} \tag{1}$$

where ρ denotes the density, $\boldsymbol{U} = (u, u_\perp)$ the velocity field, $\boldsymbol{B} = (B_x, B_\perp)$ the magnetic field and p the gas pressure. The total energy E is defined as

$$E = \rho e + \frac{1}{2}\rho |\boldsymbol{U}|^2 + \frac{1}{2}|\boldsymbol{B}|^2, \tag{2}$$

where e denotes the specific internal energy. The system is closed by an equation of state, which provides the numerical value of the gas pressure. Throughout this work we will consider an ideal gas law defined by

$$p(\rho, e) = (\gamma - 1)\rho e. \tag{3}$$

In addition to the set of equations in (1), the magnetic field satisfies the solenoidal constraint

$$\nabla \cdot \boldsymbol{B} = 0. \tag{4}$$

Solutions to the system (1) automatically satisfy this condition at all times if the initial field obeys the constraint.

2.1 Low-Mach limit of the MHD system

In order to analyze the behaviour of solutions in the low Mach regime it is of help to determine the non-dimensional form of the MHD equations. This dimensionless system can be derived by decomposing the variables into a scalar value for the units and a non-dimensional quantity, i.e.

$$\varphi = \varphi_r \hat{\varphi}. \tag{5}$$

By inserting these quantities into the dimensional system (1), we obtain

$$\begin{aligned} \frac{\partial \hat{\rho}}{\partial \hat{t}} + \hat{\nabla} \cdot (\hat{\rho}\hat{\boldsymbol{U}}) &= 0, \\ \frac{\partial (\hat{\rho}\hat{\boldsymbol{U}})}{\partial \hat{t}} + \hat{\nabla} \cdot \left[\hat{\rho}\hat{\boldsymbol{U}} \otimes \hat{\boldsymbol{U}} + \left(\frac{\hat{p}}{\hat{\mathcal{M}}^2_{\text{son}}} + \frac{1}{\hat{\mathcal{M}}^2_{\text{Alf}}}\frac{1}{2}|\hat{\boldsymbol{B}}|^2\right)\boldsymbol{I} - \frac{\hat{\boldsymbol{B}} \otimes \hat{\boldsymbol{B}}}{\hat{\mathcal{M}}^2_{\text{Alf}}}\right] &= \boldsymbol{0}, \\ \frac{\partial (\hat{\rho}\hat{E})}{\partial \hat{t}} + \hat{\nabla} \cdot \left[\left(\hat{\rho}\hat{E} + \hat{p} + \frac{\hat{\mathcal{M}}^2_{\text{son}}}{\hat{\mathcal{M}}^2_{\text{Alf}}}\frac{1}{2}|\hat{\boldsymbol{B}}|^2\right)\hat{\boldsymbol{U}} - \hat{\boldsymbol{B}}\left(\hat{\boldsymbol{B}} \cdot \hat{\boldsymbol{U}}\right)\frac{\hat{\mathcal{M}}^2_{\text{son}}}{\hat{\mathcal{M}}^2_{\text{Alf}}}\right] &= 0, \\ \frac{\partial \hat{\boldsymbol{B}}}{\partial \hat{t}} + \hat{\nabla} \cdot (\hat{\boldsymbol{U}} \otimes \hat{\boldsymbol{B}} - \hat{\boldsymbol{B}} \otimes \hat{\boldsymbol{U}}) &= \boldsymbol{0}, \end{aligned} \tag{6}$$

where $\hat{\mathcal{M}}_{\text{son}} = |U_\text{r}|/a_\text{r}$ and $\hat{\mathcal{M}}_{\text{Alf}} = |U_\text{r}|/(|B_\text{r}|/\sqrt{\rho_\text{r}})$ denote the characteristic sonic and Alfvén Mach numbers of the flow.
For analyzing the eigenstructure of the MHD system, we consider system (6) reduced to one spatial dimension. This system has seven eigenvalues

$$\lambda_{1,7} = \hat{u} \mp c_\text{f},\ \lambda_{2,6} = \hat{u} \mp c_\text{A},\ \lambda_{3,5} = \hat{u} \mp c_\text{s},\ \lambda_4 = u. \tag{7}$$

The fast magnetosonic, Alfvén and slow magnetosonic wave speeds are defined by

$$c_{\text{f,s}} = \left[\frac{1}{2}\left(a^2 + \frac{1}{\hat{\mathcal{M}}_{\text{Alf}}}\frac{|\hat{\boldsymbol{B}}|^2}{\hat{\rho}} \pm \sqrt{\left(a^2 + \frac{1}{\hat{\mathcal{M}}_{\text{Alf}}}\frac{|\hat{\boldsymbol{B}}|^2}{\hat{\rho}}\right)^2 - 4a^2c_\text{A}^2}\right)\right]^{\frac{1}{2}}, \tag{8}$$

$$c_\text{A} = \frac{1}{\hat{\mathcal{M}}_{\text{Alf}}}\frac{|\hat{B}_x|}{\sqrt{\hat{\rho}}}, \tag{9}$$

with the sound speed a defined as

$$a = \frac{1}{\hat{\mathcal{M}}_{\text{son}}}\sqrt{\frac{\gamma\hat{p}}{\hat{\rho}}}. \tag{10}$$

In this work we only consider low sonic Mach numbers, but not low Alfvén Mach numbers. Therefore, we assume $\hat{\mathcal{M}}_{\text{Alf}} = 1$ in the rest of the paper.

3 Relaxation model

Our goal is to derive a one-dimensional Riemann solver. Therefore, in the following we only consider one spatial dimension. In [5] and [6] a relaxation system is described, which leads to a 5-wave approximate Riemann solver for the MHD equations. For problems with low Mach numbers, however, this solver leads to excessive dissipation, so that the solution is poorly resolved on coarse grids (see Sect. 5). To cure this defect, we resort to a two-speed relaxation technique [3]. In this approach the relaxation speed for the normal direction is split into two different speeds and additionally a new relaxation equation for the velocity is introduced. At this point we would like to point out that the following relaxation system has a total number of three relaxation speeds (c_1, c_2 and c_a), but that we always refer to c_1 and c_2 when using the term *two-speed*. We define the following

relaxation system

$$
\begin{aligned}
\partial_t \rho + \partial_x(\rho v) &= 0,\\
\partial_t(\rho u) + \partial_x(\rho u v + \pi) &= 0,\\
\partial_t(\rho u_\perp v + \pi_\perp) &= 0,\\
\partial_t E + \partial_x\left((E+\pi)\, v + \pi_\perp \cdot u_\perp\right) &= 0,\\
\partial_t B_x + v\partial B_x &= 0,\\
\partial_t B_\perp + \partial_x\left(B_\perp v - B_x u_\perp\right) + u_\perp \partial_x B_x &= 0,\\
\partial_t(\rho\pi) + \partial_x\left(\rho\pi v\right) + c_1 c_2 \partial_x v &= \rho\frac{p-\pi}{\varepsilon},\\
\partial_t(\rho\pi_\perp) + \partial_x\left(\rho\pi_\perp v\right) + c_a^2 \partial_x v &= \rho\frac{p-\pi}{\varepsilon},\\
\partial_t(\rho v) + \partial_x\left(\rho v^2\right) + \frac{c_1}{c_2}\partial_x \pi &= \rho\frac{u-v}{\varepsilon},\\
\partial_t c_1 + v\partial_x c_1 &= 0,\\
\partial_t c_2 + v\partial_x c_2 &= 0,\\
\partial_t c_a + v\partial_x c_a &= 0.
\end{aligned}
\tag{11}
$$

The two pressure variables π and $\pi_\perp$ are defined in equilibrium by

$$
\pi = p + \frac{1}{2}|B_\perp|^2 - \frac{1}{2}B_x^2 \quad \text{and} \quad \pi_\perp = -B_x B_\perp. \tag{12}
$$

As long as the relaxation speeds c_1, c_2 and c_a satisfy the stability conditions

$$
\begin{aligned}
\frac{1}{\rho} - \frac{B_x^2}{c_a^2} \geq 0, \quad c_1 c_2 - \rho^2 a^2 \geq 0,\\
|B_\perp| \leq \left(c_1 c_2 - \rho^2 a^2\right)\left(\frac{1}{\rho} - \frac{B_x^2}{c_a^2}\right), \quad c_1 \geq c_2,
\end{aligned}
\tag{13}
$$

solutions of the relaxation system are viscous approximations of the solutions of the original MHD system. The homogeneous system $(11)_{\varepsilon=\infty}$ is hyperbolic and admits the eigenvalues

$$
\lambda_f^{\pm} = v \pm max(c_a, c_1), \quad \lambda_s^{\pm} = v \pm min(c_a, c_1), \quad \lambda_v = v. \tag{14}
$$

All characteristic fields are linearly degenerate and the Riemann invariants for the different waves are given as follows

$$
\begin{aligned}
v-\frac{c_1}{\rho}:\quad & v-\frac{c_1}{\rho},\ u-\frac{c_2}{\rho},\ \pi+\frac{c_1c_2}{\rho},\ \frac{B_\perp}{\rho}, u_\perp,\ B_x,\ \pi_\perp,\ c_1,\ c_2,\ c_a,\\
& \frac{2c_1c_2-c_2^2-2c_2\rho(v-u)+\rho\left(2\pi+|B_\perp|^2+B_x^2+2\rho e\right)}{2\rho^2},\\
v-\frac{c_a}{\rho}:\quad & \pi_\perp+c_au_\perp,\ B_\perp-\frac{\rho u_\perp B_x}{c_a},\ e+\frac{c_a^2u_\perp^2+2c_au_\perp(B_xB_\perp+\pi_\perp)-\rho B_x^2u_\perp^2}{2c_a^2},\\
& \rho,\ u,\ B_x,\ \pi,\ v,\ c_1,\ c_2,\ c_a,\\
v:\quad & v,\ u_\perp,\ \pi,\ \pi_\perp,\\
v+\frac{c_a}{\rho}:\quad & \pi_\perp-c_au_\perp,\ B_\perp+\frac{\rho u_\perp B_x}{c_a},\ e+\frac{c_a^2u_\perp^2-2c_au_\perp(B_xB_\perp+\pi_\perp)-\rho B_x^2u_\perp^2}{2c_a^2},\\
& \rho,\ u,\ B_x,\ \pi,\ v,\ c_1,\ c_2,\ c_a,\\
v+\frac{c_1}{\rho}:\quad & v+\frac{c_1}{\rho},\ u+\frac{c_2}{\rho},\ \pi+\frac{c_1c_2}{\rho},\ \frac{B_\perp}{\rho},\ u_\perp,\ B_x,\ \pi_\perp,\ c_1,\ c_2,\ c_a,\\
& \frac{2c_1c_2-c_2^2+2c_2\rho(v-u)+\rho\left(2\pi+|B_\perp|^2+B_x^2+2\rho e\right)}{2\rho^2}.
\end{aligned}
$$

Let us now introduce the state vector

$$
W=(\rho,\rho u,\rho u_\perp,E,B_x,B_\perp,\rho\pi,\rho\pi_\perp,\rho v,c_1,c_2,c_a)^T. \tag{15}
$$

The solution to the Riemann problem associated with system $(11)_{\varepsilon=\infty}$ given by

$$
W_0(x)=\begin{cases}W^L, & x<0,\\ W^R, & x>0,\end{cases} \tag{16}
$$

consists of six constant states. Therefore the Riemann solver $W_{\mathcal{R}}(x/t;W^L,W^R)$ has the structure

$$
W_{\mathcal{R}}(x/t;W^L,W^R)=\begin{cases}W^L, & \frac{x}{t}<\lambda_f^-,\\ W^{L*}, & \lambda_f^-<\frac{x}{t}<\lambda_s^-,\\ W^{L**}, & \lambda_s^-<\frac{x}{t}<\lambda_v,\\ W^{R**}, & \lambda_v<\frac{x}{t}<\lambda_s^+,\\ W^{R*}, & \lambda_s^+<\frac{x}{t}<\lambda_f^+,\\ W^R, & \lambda_f^+<\frac{x}{t}.\end{cases} \tag{17}
$$

The intermediate states can be derived using the invariants from above. Due to their large number, we will not list the intermediate states here. The definition of the relaxation speeds is given in Sect. 4.

4 Definition of the relaxation speeds and the low Mach property

In line with the definitions of the relaxation speeds for the one-speed solver in [6], we define the speeds for the two-speed solver for $\alpha = 1, 2$ by

$$\begin{aligned} c_\alpha^L &= \rho^L a_{0,\alpha}^L + \beta\rho^L \left((v^L - v^R)_+ + \frac{(\pi^R - \pi^L)_+}{\rho^L a_q^L + \rho^R a_q^R} \right), \\ c_\alpha^R &= \rho^R a_{0,\alpha}^R + \beta\rho^R \left((v^L - v^R)_+ + \frac{(\pi^L - \pi^R)_+}{\rho^L a_q^L + \rho^R a_q^R} \right), \\ c_a^L &= \sqrt{\frac{\rho^L}{x^L}\left(B_x^2 + |B_x B_\perp^L|\right)}, \quad c_a^R = \sqrt{\frac{\rho^R}{x^R}\left(B_x^2 + |B_x B_\perp^R|\right)}, \end{aligned} \tag{18}$$

with

$$a_{0,1}^2 = \frac{1}{\min\left(\phi^2, 1\right)} a^2 + \frac{|B_\perp|^2 + |B_x B_\perp|}{\rho x}, \tag{19}$$

$$a_{0,2}^2 = \min\left(\phi^2, 1\right) a^2 + \frac{|B_\perp|^2 + |B_x B_\perp|}{\rho x}, \tag{20}$$

$$a_q^2 = \min\left(\phi^2, 1\right) a^2 + \frac{|B_\perp|^2 + |B_x B_\perp|}{\rho}. \tag{21}$$

For more details on the definitions of the used quantities, we refer the reader to [6]. We want to point out that for $\phi = 1$, we get $c_1 = c_2$ and consequently the speeds coincide with the definitions in the one-speed solver. However, to get the desired effect of the two-speed approach, we set $\phi = \hat{\mathcal{M}}_{son}$. As a consequence, taking into account the results of Sect. 2.1, the speeds scale in this case by

$$c_1 = \mathcal{O}(1/\hat{\mathcal{M}}_{son}^2) \quad \text{and} \quad c_2 = \mathcal{O}(1). \tag{22}$$

This rescaling by the Mach number is essential to prevent excessive numerical dissipation in the low Mach regime. This becomes clear when looking at the intermediate state of the pressure π given by

$$\pi^* = \frac{c_2^R \pi^L + c_2^L \pi^R - c_2^L c_2^R (v^R - v^L)}{c_2^L + c_2^R}. \tag{23}$$

This state can be viewed as a central flux of the left and right pressure combined with a dissipation term including the velocity difference $v^R - v^L$. Thanks to the rescaling, c_2 is of order $\mathcal{O}(1)$, which keeps the amount of dissipation in the pressure independent of the Mach number. For the one-speed solver, on the other hand, the relaxation speed $c = c_1 = c_2$ scales with $\mathcal{O}(1/\hat{\mathcal{M}}_{son})$. Thus, in the low Mach regime, the dissipation term becomes the dominant part of the momentum flux, causing the dissipation to increase with decreasing Mach number. The rescaling in the two-speed approach prevents this behaviour.

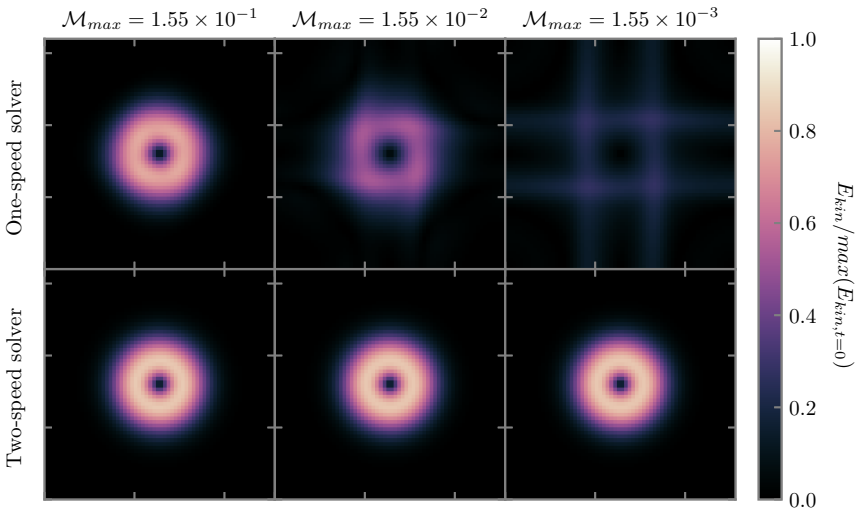

Fig. 1. Distribution of the kinetic energy for different maximum Mach numbers $\mathcal{M}_{max}$ after one full turnover

5 Numerical results

The one-dimensional approximate Riemann solver (17) is incorporated into a second order two-dimensional unsplit finite volume method, that uses a standard linear reconstruction with minmod-limiter. In order to keep the divergence of the magnetic field to machine precision, the scheme is combined with a second order staggered constrained transport method [10]. For time discretisation, the explicit method of Heun is used. The CFL condition relies on the maximum wave speed derived from (14). For comparison, we also show results of the one-speed solver, in which the relaxation speeds are not rescaled with the Mach number and thus we set $c_1 = c_2$.

5.1 Stationary vortex

We start with a stationary vortex that can be set up with different maximum Mach numbers [1]. We compute the numerical solution on a 64×64 grid and evaluate the kinetic energy distribution after one full turnover. The results for different maximum Mach numbers $\mathcal{M}_{max}$ are shown in Fig. 1. Clearly, the one-speed solver introduces too much artifical dissipation, so that the loss of kinetic energy is quite large. With the two-speed method, on the other hand, the loss of kinetic energy is independent of the Mach number.

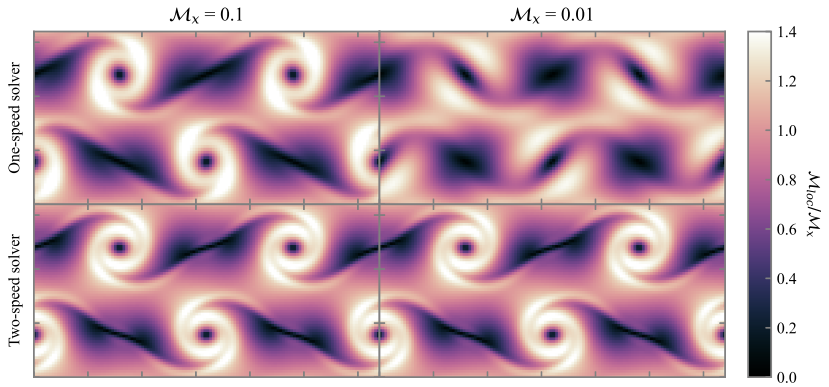

Fig. 2. Distribution of the local sonic Mach number relative to $\mathcal{M}_x$ at final time t_f

5.2 Kelvin Helmholtz instability

A more sophisticated test is the magnetised version of the Kelvin Helmholtz instability [9]. This test is set up with different maximum Mach number of the horizontal flow denoted by $\mathcal{M}_x$. We compute the solution on a 128×64 grid until the final time $t_f = 0.8/\mathcal{M}_x$. Fig. 2 shows the distribution of the local sonic Mach number $\mathcal{M}_{loc}$ relative to $\mathcal{M}_x$. The test again shows that the two-speed solver introduces significantly less numerical dissipation and can therefore resolve the details of the solution much better.

6 Summary

In this work, we have built an approximate Riemann solver using the two-speed technique, which gives accurate solutions even in the low Mach regime. Typically, relaxation-based Riemann solvers satisfy a discrete entropy inequality when the subcharacteristic condition is satisfied. The goal of future work will be to prove such a result for the solver described here. Furthermore, it would be interesting to investigate whether the two-speed approach can also be applied or extended to the low Alfvén Mach regime.

Acknowledgments

CB acknowledges the support by the German Research Foundation (DFG) under the project no. KL 566/22-1

References

1. Berberich, J.P., Chandrashekar, P., Klingenberg, C.: High order well-balanced finite volume methods for multi-dimensional systems of hyperbolic balance laws. Computers & Fluids, 219:104858 (2021)
2. Birke, C., Chalons, C., Klingenberg, C.: A low Mach two-speed relaxation scheme for the compressible Euler equations with gravity. arXiv:2112.02986v2 (2022)
3. Bouchut, F., Chalons, C., Guisset, S.: An entropy satisfying two-speed relaxation system for the barotropic Euler equations: application to the numerical approximation of low Mach number flows. Numerische Mathematik, 145:35–76 (2020)
4. Bouchut, F., Franck, E., Navoret, L.: A low cost semi-implicit low-Mach relaxation scheme for the full Euler equations. Journal of Scientific Computing, 83(1):24, 2020.
5. Bouchut, F., Klingenberg, C., Waagan, K.: A multiwave approximate Riemann solver for ideal MHD based on relaxation. I: theoretical framework. Numerische Mathematik, 108:7–42 (2007)
6. Bouchut, F., Klingenberg, C., Waagan, K.: A multiwave approximate Riemann solver for ideal MHD based on relaxation II: numerical implementation with 3 and 5 waves. Numerische Mathematik, 115:647–679 (2010)
7. Chen, W., Wu, K., Xiong, T.: High Order Asymptotic Preserving Finite Difference WENO Schemes with Constrained Transport for MHD Equations in All Sonic Mach Numbers. arXiv:2211.16655 (2022)
8. Dumbser, M., Balsara, D.S., Tavelli, M., Fambri, F.: A divergence-free semi-implicit finite volume scheme for ideal, viscous, and resistive magnetohydrodynamics. International Journal for Numerical Methods in Fluids, 89(1-2):16–42 (2019)
9. Leidi, G., Birke, C., Andrassy, R., Higl, J., Edelmann, P.V.F., Wiest, G., Klingenberg, C., Röpke, F.K.: A finite-volume scheme for modeling compressible magnetohydrodynamic flows at low Mach numbers in stellar interiors. Astronomy & Astrophysics, 668, no. A143 (2022)
10. Gardiner, T.A., Stone, J.M.: An unsplit Godunov method for ideal MHD via constrained transport. Journal of Computational Physics, 205(2):509–539 (2005)
11. Minoshima, T., Miyoshi, T.: A low-dissipation HLLD approximate Riemann solver for a very wide range of Mach numbers. Journal of Computational Physics, 446:110639 (2021)